

Electronic structure of the quasi-one-dimensional halogen-bridged Ni complexes [Ni(chxn)₂X]X₂ (X=Cl, Br) and related Ni compounds

H. Okamoto, Y. Shimada, and Y. Oka

Research Institute for Scientific Measurements, Tohoku University, Sendai 980, Japan

A. Chainani and T. Takahashi

Department of Physics, Faculty of Science, Tohoku University, Sendai 980, Japan

H. Kitagawa and T. Mitani

Japan Advanced Institute of Science and Technology, Ishikawa 923-12, Japan

K. Toriumi

Department of Material Science, Himeji Institute of Technology, Harima Science Park City, Hyogo 678-12, Japan

K. Inoue, T. Manabe, and M. Yamashita

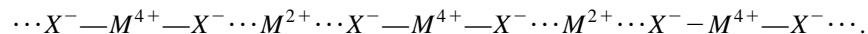
Graduate School of Human Informatics, Nagoya University, Nagoya 464-01, Japan

(Received 15 April 1996)

The electronic structure of the one-dimensional Ni complexes, [Ni(chxn)₂X]X₂ (X=Cl, Br; (chxn)=1*R*,2*R*-cyclohexanediamine), is studied together with the discrete Ni complexes, [NiX₂([14]aneN₄)]ClO₄ (X=Cl; Br; ([14]aneN₄)=1,4,8,11-tetraazacyclotetradecane), using optical spectroscopy, x-ray photoelectron spectroscopy (XPS) and Auger electron spectroscopy. The optical spectra show that the Br compounds have a smaller gap as compared with the Cl compounds. An analysis using a simple X-Ni-X trimer model on the optical spectra and the Ni 2*p* XP spectra yields quantitative estimates for the charge transfer (CT) energy Δ and the transfer energy T for discrete and one-dimensional Ni complexes. The analysis on the Ni *L*VV Auger spectra in conjunction with the valence XP spectra indicates that the average on-side *d-d* Coulomb energy U in the one-dimensional and discrete Ni complexes is about 5 eV, quite similar to the case of the Ni dihalides. The obtained results demonstrate that the one-dimensional Ni complexes are CT insulators. We discuss the differences in the electronic structures of the one-dimensional Ni complexes compared with the Ni dihalides and the one-dimensional Pt complexes on the basis of the estimated parameter values of Δ , T , and U . [S0163-1829(96)07335-3]

I. INTRODUCTION

In recent years, the one-dimensional (1D) halogen (*X*)-bridged transition-metal (*M*) complexes (or, equivalently, the *MX* chain compounds) have been attracting much attention as a good target material to investigate the properties of the 1D electronic state under the influence of both the strong electron-lattice (*e-l*) interaction and electron-electron correlation.¹⁻⁴ In *MX* chain compounds, the electronic structure of the 1D chain is composed of the half-filled *d*_{z²} orbitals of metals, and the filled *p*_z orbitals of halogens. So far, studies have concentrated on the complexes with *M*=Pt and Pd, for which it is established that the bridging halogen ion deviates from the midpoint between the neighboring metal ions due to the site-diagonal-type *e-l* interactions and the commensurate charge-density wave (CDW) is stabilized even at room temperature as shown below.



In complexes with *M*=Pt or Pd, the energy level of the *p*_z orbital of halogens is much lower than that of the *d*_{z²} orbital of metals.⁵ Therefore, their electronic structures are described essentially by the 1D Peierls-Hubbard model, in which only the *d*_{z²} orbitals are taken into account and the contribution of the *p*_z orbitals is effectively incorporated into the supertransfer energy between the *d*_{z²} orbitals of the neighboring metal ions.⁴ In these complexes, electronic structures of fundamental excitations such as excitons, solitons, and polarons, and their dynamical properties, have been clarified from both experimental⁶⁻¹⁰ and theoretical points of view.¹¹⁻¹⁷

In contrast to Pt and Pd complexes, complexes with *M*=Ni such as [Ni(chxn)₂X]X₂ (X=Cl, Br; (chxn)=1*R*,2*R*-cyclohexane-diamine) have a regular chain structure composed of Ni³⁺ ions and X⁻ ions shown below.^{2,18,19}



Lattice distortions related to Peierls or spin-Peierls mechanisms have not been observed even at low temperatures. These complexes are found to be insulating, suggesting the importance of electron-electron interactions between $3d$ electrons. Hence this kind of material may be regarded as a prototype of a strongly correlated 1D electron (spin) system. In fact, the magnetic susceptibility χ of $[\text{Ni}(\text{chxn})_2\text{Br}]\text{Br}_2$ has a finite value even at low temperatures, which is scarcely dependent on temperature.² Such a behavior for χ has been tentatively interpreted by using the 1D Heisenberg ($s = \frac{1}{2}$) model with a large antiferromagnetic exchange interaction J (~ 3600 K).² However, the natures of the electronic and spin states seem not to be fully understood.

In order to investigate the electronic structure of these strongly correlated electronic systems, high-energy spectroscopy is a powerful tool. In fact, not only the simple divalent transition-metal oxides and halides, but also the perovskites of Cu, Ni and other transition-metal oxides, have been extensively studied by high-energy electron spectroscopy [x-ray photoemission spectroscopy (XPS), x-ray absorption spectroscopy, ultraviolet photoemission spectroscopy, bremsstrahlung isochromat spectroscopy, etc.]. Studies of simple Ni dihalides such as NiX_2 ($X = \text{F}, \text{Cl}, \text{Br}, \text{I}$) have shown that the band gaps are of a charge-transfer (CT) type,^{20,21} determined by a halogen-to-metal CT energy Δ . In these compounds, Δ is smaller than U , the on-site d - d Coulomb interaction energy, and the magnitude of Δ has been found to depend on the choice of halogens following the expected chemical trend.²¹

The target material of the present study is $[\text{Ni}(\text{chxn})_2\text{X}]\text{X}_2$ ($X = \text{Cl}, \text{Br}$). (Hereafter, these complexes are called 1D Ni complexes.) As compared with NiX_2 , important features of electronic states of the 1D Ni complexes are summarized as follows. (1) Ni is trivalent $[(t_{2g})^6(e_g)^1]$. (2) The electronic states are purely one-dimensional. (3) The organic ligand molecules (chxn) coordinate the Ni ions, probably leading to a strong crystal field. It is interesting to investigate whether the CT energy and/or the electron correlation might be modified in the 1D Ni complexes.

In this paper, we report the valence XP spectra, the Ni $2p$ XP spectra, and the Ni LVV Auger spectra, together with the optical-absorption spectra of the 1D Ni complexes; $[\text{Ni}(\text{chxn})_2\text{X}]\text{X}_2$ ($X = \text{Cl}, \text{Br}$). These measurements were also performed on the NiX_2 and $[\text{NiX}_2([\text{14}] \text{aneN}_4)]\text{ClO}_4$ ($X = \text{Cl}, \text{Br}$; $([\text{14}] \text{aneN}_4) = 1,4,8,11$ -tetraazacyclotetradecane) compounds for reference. The latter materials are composed of discrete $X^- \text{-Ni}^{3+} \text{-X}^-$ units. (Hereafter, these complexes are called discrete Ni complexes.) The parameter U has been evaluated from a comparison between the Ni LVV Auger spectra and the self-convolution of the valence-band XP spectra. Δ and the transfer energy T between the p_z orbital and the d_{z^2} orbital have been obtained from an analysis of the satellite structures in the Ni $2p$ XP spectra and the optical gap energies. From the results, we discuss the electronic structures of the 1D Ni complexes $[\text{Ni}(\text{chxn})_2\text{X}]\text{X}_2$ ($X = \text{Cl}, \text{Br}$), which will be compared with those of NiX_2 . Moreover, the difference in the ground states between the 1D Ni complexes and the isomorphous 1D Pt (or Pd) complexes in the CDW phase will be elucidated on the basis of the difference of the electronic structures, namely, Δ and U .

II. EXPERIMENT

Single crystals of the Ni complexes, $[\text{Ni}(\text{chxn})_2\text{X}]\text{X}_2$ ($X = \text{Cl}, \text{Br}$) and $[\text{NiX}_2([\text{14}] \text{aneN}_4)]\text{ClO}_4$ ($X = \text{Cl}, \text{Br}$) were prepared according to the literature.^{18,19,22} NiX_2 ($X = \text{Cl}$ and Br) samples were commercially obtained.

The measurements of the XP and Auger spectra were performed using a ESCALAB MK II (VG Scientific Co.) photoelectron spectrometer with Mg $K\alpha$ ($h\nu = 1253.6$ eV) or Al $K\alpha$ ($h\nu = 1486.6$ eV) as an excitation light source. In these measurements, all samples were ground into powder form in a N_2 -gas-filled glovebox attached to the preparation chamber, and inserted into the high-vacuum chamber without exposing to air. The base pressure of the analysis chamber was 10^{-10} -Torr range. The excitation light was operated at low power, because the samples degraded on prolonged exposure at high incident power, as observed by the broadening of the Ni $2p$ core-level spectra. The Fermi level of the sample was determined by referring to that of silver sample.

For the measurements of polarized reflection spectra, a halogen-tungsten incandescent lamp was used. Light from the lamp was focused by a concave mirror on the entrance slit of a 25-cm grating monochromator (JASCO GD-25). The monochromatic light from the exit slit was passed through a polarizer, and was focused on the specific surface of a single-crystal sample by using an optical microscope. Reflected light from the sample was focused by a concave mirror on the detector (a PbS cell or a photomultiplier tube). For measurements of the absorption spectra, the ground powder samples were dispersed in liquid paraffin.

III. CRYSTAL STRUCTURES

Figure 1(a) shows the crystal structure of $[\text{Ni}(\text{chxn})_2\text{Br}]\text{Br}_2$ viewed along the \mathbf{a} axis.¹⁸ The four N atoms of amino groups in two (chxn) molecules coordinate a Ni^{3+} ion. The Ni^{3+} (chxn)₂ units bridged by the Br^- ions are stacked along the \mathbf{b} axis (the chain axis). The neighboring $\text{Ni}(\text{chxn})_2$ moieties on the same chain are linked by the four $\text{NH}\cdots\text{Br}^-\cdots\text{HN}$ intrachain hydrogen bonds which are drawn by the dashed lines in Fig. 1(a). The hydrogen-bond network extends over the chains, forming a 2D structure parallel to the bc plane. But the electron wave function of a Ni-Br chain does not overlap with that of the neighboring chains, and the electronic state is purely one-dimensional. The crystal structure of $[\text{Ni}(\text{chxn})_2\text{Cl}]\text{Cl}_2$ (Ref. 19) is the same as that of $[\text{Ni}(\text{chxn})_2\text{Br}]\text{Br}_2$.

The molecular structure of the discrete Ni^{3+} complex, $[\text{NiBr}_2([\text{14}] \text{aneN}_4)]\text{ClO}_4$, is shown in Fig. 1(b).²³ The four N atoms of a macrocyclic molecule ($[\text{14}] \text{aneN}_4$) coordinate a Ni^{3+} ion. A $\text{NiBr}_2([\text{14}] \text{aneN}_4)$ unit is completely isolated from the neighboring ones by the counter anions $(\text{ClO}_4)^-$. The crystal structure of $[\text{NiCl}_2([\text{14}] \text{aneN}_4)]\text{ClO}_4$ (Ref. 24) is isomorphous with that of $[\text{NiBr}_2([\text{14}] \text{aneN}_4)]\text{ClO}_4$.

Ni dihalides have a cadmium chloride structure. The Ni^{2+} ions are located in a distorted octahedron formed by the nearest-neighbor halogen ions. These materials are considered layered compounds, with the Ni layers alternating with a double layer of halogen atoms.

In Table I, the interatomic distances Ni-X and Ni-N, are listed for the Ni compounds discussed in this paper.^{18,19,21,24} The Ni-X distances are quite similar for the three types of

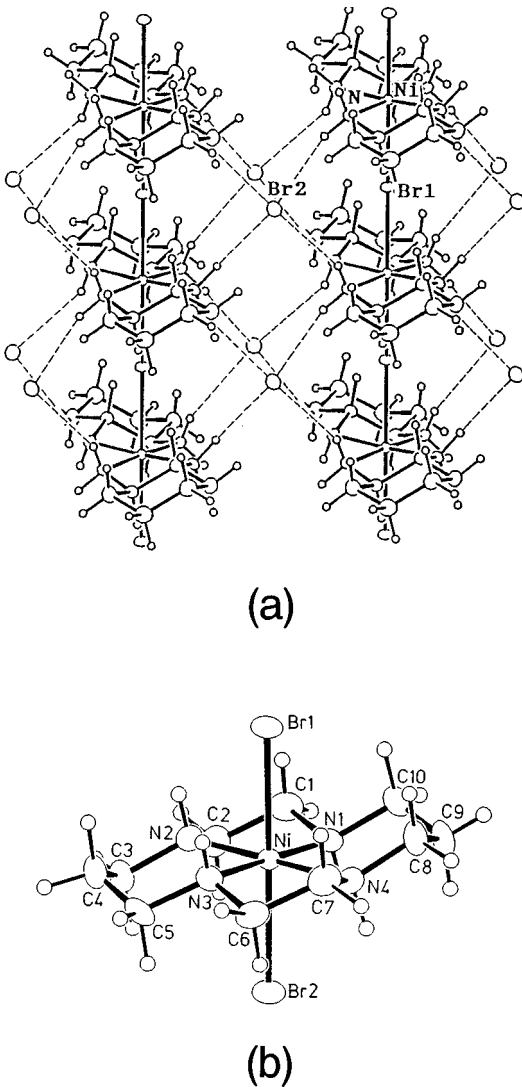


FIG. 1. (a) Crystal structure of $[\text{Ni}(\text{chxn})_2\text{Br}]\text{Br}_2$ viewed along the **a** axis. The 1D Ni-Br chain is along the **b** axis. (b) The molecular structure of $\text{NiBr}_4([\text{14}]\text{aneN}_4)$ in the $[\text{NiBr}_2([\text{14}]\text{aneN}_4)]\text{ClO}_4$ complex.

compounds (2.45–2.46 Å for $X=\text{Cl}$, and 2.58–2.62 Å for $X=\text{Br}$). The distance between a Ni ion and the nearest-neighbor C atom is large (~ 2.8 Å) for both the discrete and 1D Ni complexes. The sp^3 hybridized orbitals of the C atom form σ bonds with neighboring C, H, and N atoms, and therefore have negligible overlaps with the d orbitals of the Ni ion.

TABLE I. Comparison of the averaged bond distances (Å).

	Ni-X	Ni-N	Ref.
$[\text{NiCl}_2([\text{14}]\text{aneN}_4)]\text{ClO}_4$	2.452	1.970	24
$[\text{NiBr}_2([\text{14}]\text{aneN}_4)]\text{ClO}_4$	2.616	1.971	18
$[\text{Ni}(\text{chxn})_2\text{Cl}]\text{Cl}_2$	2.447	1.944	19
$[\text{Ni}(\text{chxn})_2\text{Br}]\text{Br}_2$	2.578	1.944	18
NiCl_2	2.46		21
NiBr_2	2.58		21

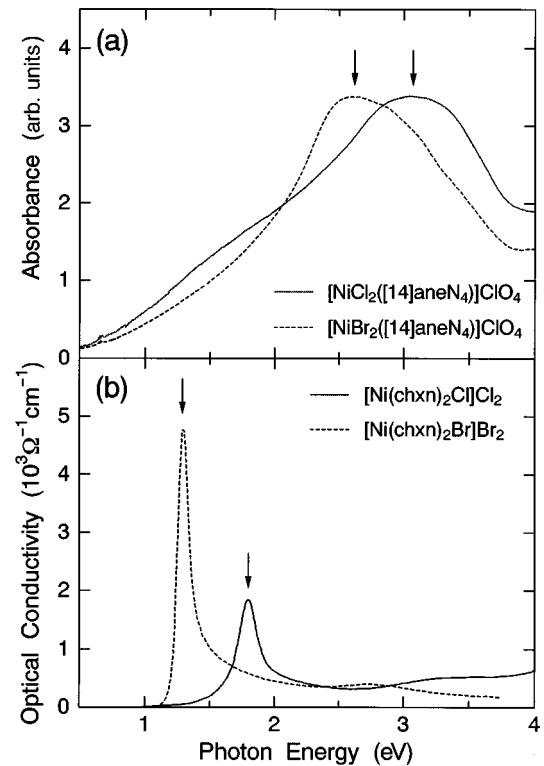


FIG. 2. (a) Absorption spectra of $[\text{NiX}_2([\text{14}]\text{aneN}_4)]\text{ClO}_4$ ($X=\text{Cl}, \text{Br}$) for powder samples. (b) Optical conductivity spectra of $[\text{Ni}(\text{chxn})_2\text{X}]\text{X}_2$ ($X=\text{Cl}, \text{Br}$) for the single crystals with $\mathbf{E}||\mathbf{b}$ (chain axis).

IV. EXPERIMENTAL RESULTS

A. Optical-absorption spectra

The absorption spectra of the powder samples of discrete Ni complexes, and the optical conductivity spectra of single crystals of 1D Ni complexes, are presented in Figs. 2(a) and 2(b), respectively. Optical conductivity spectra were obtained by the Kramers-Kronig transformation from the polarized reflectivity spectra, with the electric vector \mathbf{E} parallel to the chain axis \mathbf{b} ($\mathbf{E}||\mathbf{b}$). In the absorption spectra of the discrete Ni complexes, weak structures are observed around 1.6 eV, which can be attributed to the intraatomic $d-d$ transition of Ni^{3+} ions.²² This transition is weakly allowed in the distorted octahedron structure, where the Ni-X bonds are slightly tilted from the normal to the NiN_4 plane. Strong absorption bands around 3.1 eV for $X=\text{Cl}$ and around 2.6 eV for $X=\text{Br}$ are assigned to the halogen to Ni CT transition ($X^-, \text{Ni}^{3+} \rightarrow X^0, \text{Ni}^{2+}$). On the other hand, in 1D Ni complexes, absorption peaks corresponding to the gap energies are observed at much lower energies (~ 1.8 eV for $X=\text{Cl}$ and 1.3 eV for $X=\text{Br}$). These bands were found to be polarized parallel to the chain axis \mathbf{b} , and may be assigned to the intermetallic transition corresponding to the Hubbard gap ($\text{Ni}^{3+}, \text{Ni}^{3+} \rightarrow \text{Ni}^{4+}, \text{Ni}^{2+}$) or the halogen to Ni CT transition. In our previous papers,^{2,3,25} we had tentatively adopted the former assignment, but the results presented in this paper demonstrate the latter assignment to be appropriate as discussed in Sec. V. The energies E_{CT} of the absorption peaks indicated by the arrows in Fig. 2 are listed in Table II.

TABLE II. The optical gap energies E_{CT} , the peak energies of the main line E_{main} , and the satellite E_{sat} in the Ni $2p_{3/2}$ XP spectra, the splitting of the $2p_{3/2}$ lines $E_s (= E_{sat} - E_{main})$ and the intensity ratio I_{sat}/I_{main} for the discrete and 1D Ni complexes.

	E_{CT} (eV)	E_{main} (eV)	E_{sat} (eV)	E_s (eV)	I_{sat}/I_{main}
$[\text{NiCl}_2([\text{14}]ane\text{N}_4)]\text{ClO}_4$	3.07	855.2	861.9	6.7	0.55 ± 0.1
$[\text{NiBr}_2([\text{14}]ane\text{N}_4)]\text{ClO}_4$	2.62	855.0	862.0	7.0	0.55 ± 0.1
$[\text{Ni}(\text{chxn})_2\text{Cl}]\text{Cl}_2$	1.80	855.0	862.7	7.7	0.65 ± 0.1
$[\text{Ni}(\text{chxn})_2\text{Br}]\text{Br}_2$	1.28	854.7	862.7	8.0	0.65 ± 0.1

B. Valence-band XP spectra

In Fig. 3, we present the valence-band XP spectra of the six Ni compounds, which were obtained using Mg $K\alpha$ radiation. In the spectra for the discrete and 1D Ni complexes, a broad peak centered at 3–4 eV binding energy is observed. Both Ni $3d$ and halogen $3p$ (Cl) or $4p$ (Br) electrons will contribute to the XP intensities in this energy region. Since the XP cross section of the Ni $3d$ electrons is comparatively larger than those of Cl $3p$ and Br $4p$ electrons for the Mg $K\alpha$ radiation,²⁶ the broad peak at 3–4 eV can be considered to have a dominantly $3d$ character. The spectra for NiX_2 are broader compared with the discrete and 1D Ni complexes.

C. Ni $2p$ XP spectra

The Ni $2p$ XP spectra obtained using Mg $K\alpha$ radiation are shown in Fig. 4. The spectra of NiX_2 are in good agreement with those previously reported,²¹ exhibiting a main line and two satellite structures in both Ni $2p_{3/2}$ and $2p_{1/2}$ regions. On the other hand, in discrete and 1D Ni complexes, only one satellite structure is observed. In Table II, we list

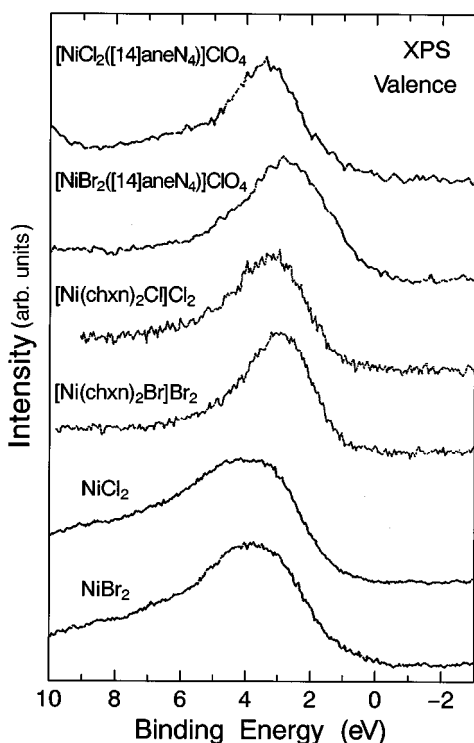


FIG. 3. Valence-band XP spectra of the Ni compounds measured with Mg $K\alpha$ radiation at room temperature.

the binding energies (E_{main} and E_{sat}) and the splitting (E_s) of the two $2p_{3/2}$ lines, and the satellite intensities relative to the main line I_{sat}/I_{main} for the discrete and 1D Ni complexes. I_{sat}/I_{main} was determined from the area under the curve after subtracting a linear background. In the estimations of I_{sat}/I_{main} , there are some ambiguity (see Table II), since the satellite structures are considerably broadened. It has been reported that the $2p_{1/2}$ spectra are seriously affected by the strong interference effects,²¹ and hence we restrict our discussion to the $2p_{3/2}$ lines in this paper.

D. Ni LVV Auger spectra

In order to study electron-electron correlation between the $3d$ electrons U , the Ni LVV Auger spectra have been measured. The results are shown in Fig. 5. The Auger spectra for NiX_2 were obtained by Mg $K\alpha$ radiation, while those for the 1D and discrete Ni complexes were obtained by Al $K\alpha$ radiation, since the strong N $1s$ XP line appears in the Auger

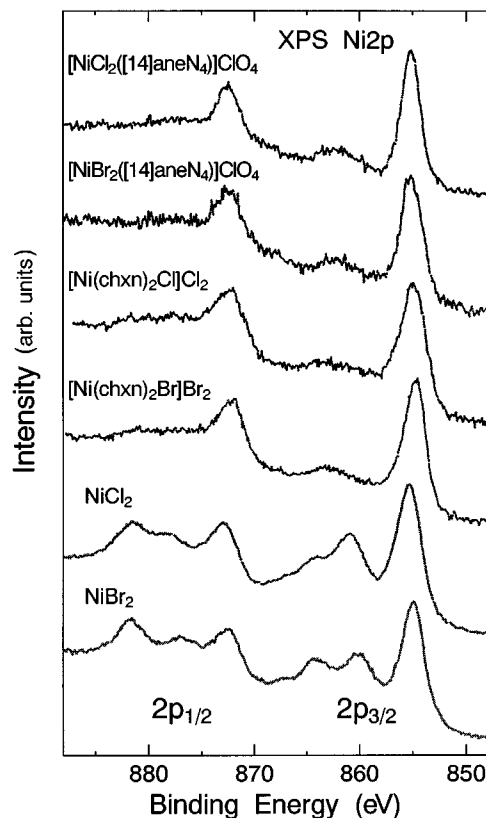


FIG. 4. Ni $2p$ XP spectra of the Ni compounds measured with Mg $K\alpha$ radiation at room temperature.

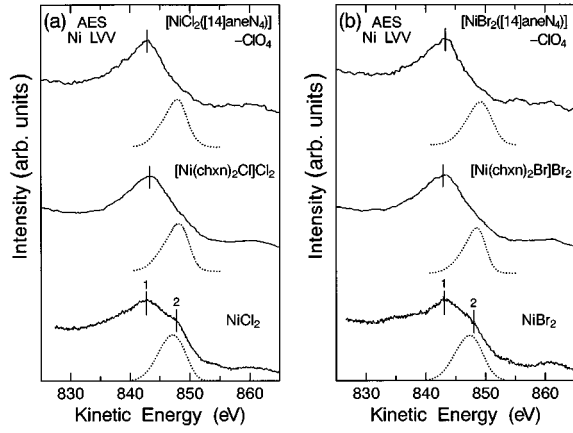


FIG. 5. Ni *LVV* Auger spectra of $[\text{NiX}_2([\text{14}] \text{aneN}_4)]\text{ClO}_4$ and $[\text{Ni}(\text{chxn})_2\text{X}]\text{X}_2$ measured with Al $K\alpha$ radiation, and of NiX_2 measured with Mg $K\alpha$ radiation: (a) for $X=\text{Cl}$ and (b) for $X=\text{Br}$. All measurements were performed at room temperature. The dotted lines are the self-convolution of the valence-band XP spectra shown in Fig. 3.

spectral region with the excitation of the Mg $K\alpha$ radiation. For NiX_2 , two structures labeled 1 and 2 are clearly identified. On the other hand, for the other four complexes, the spectra exhibit a single peak, the kinetic energy of which is almost equal to that of the lower kinetic-energy structure 1 in NiX_2 . In Table III, the kinetic energies of the observed Auger lines are listed. From the energy positions of these structures, magnitude of U , the average on-site Coulomb energy can be evaluated, as discussed in Sec. V.

V. DISCUSSIONS

In the Ni compounds investigated here, the contribution of the electron-electron correlation U is essential for opening the large gap energies. As for U , the Ni *LVV* Auger spectra give important information.

In order to characterize the origin of the structures in the Ni *LVV* Auger spectra in Fig. 5, we numerically calculated the self-convolution of the valence-band XP spectra as plotted by the dotted lines, which correspond to the two-hole final state spectrum of the interatomic Auger process in absence of the electron (hole) correlation.^{27–29} The zero of the two-hole final-state spectrum has been shifted by the binding energy of the main peak of the Ni $2p_{3/2}$ core level (E_{main} in Table II). The peak energies (E'_2) of the self-convolution

spectra are listed in Table III. As seen in Fig. 5 for NiX_2 , the structure around 848 eV is due to the presence of two uncorrelated holes, and consequently the structure around 843 eV is attributable to the two correlated hole final states. The values of U for NiX_2 are estimated to be about 5 eV from the separation of the two structures, which are listed in Table III. A similar comparison shows that the features in the Auger electron spectra of the 1D and discrete Ni complexes are attributable to the intraatomic Auger process under the influence of the correlation U . From the difference between the peak energy of the observed Auger line (E_1) and that of the self-convolution spectrum (E'_2), U is estimated to be about 5 eV for both the discrete Ni complexes and the 1D Ni complexes as listed in Table III.

The fact that Auger lines due to the interatomic process are not observed in 1D Ni or discrete Ni complexes suggests that p - d hybridization would be smaller compared with that in NiX_2 , leading to a suppression of spectral weight for the interatomic process.

As seen in Fig. 2 (or Table II), the optical gap energies of the 1D Ni complexes are much smaller than the values of U (~ 5 eV) estimated from the Auger spectra. This suggests that these optical gaps are not due to the Hubbard gap but to the charge-transfer gap essentially determined by Δ , similarly to the case of NiX_2 . The change of Δ is responsible for the difference in the gap energies between the complexes with $X=\text{Br}$ and Cl .

We next discuss the Ni $2p$ core-level satellite structures. As previously reported in detail by Zaanen, Westra, and Sawatzky,²¹ the appearance of the two satellite structures in NiCl_2 and NiBr_2 is related to the fact that both the ground and excited (final) states are composed of $|d^8\rangle$, $|d^9\bar{L}\rangle$, and $|d^{10}\bar{L}^2\rangle$ states by the effect of the p - d hybridization. Here \bar{L} indicates a hole in the halogen p orbital. In contrast, NiF_2 shows only one satellite to the main peak. As NiF_2 is more ionic compared with NiCl_2 and NiBr_2 , the ground state will be dominated by $|d^8\rangle$ and $|d^9\bar{L}\rangle$ contributions leading to a single satellite structure.²¹ This is also the case for 1D and discrete Ni complexes, with the observed spectra exhibiting only one satellite structure around 862 eV (see Fig. 4). In these complexes, the p - d hybridization occurs between the d_{z^2} orbitals of the Ni ions and the p_z orbitals of the halogen ions. The $d_{x^2-y^2}$ orbitals of the Ni ions have negligible overlap with the p orbitals of halogen ions. It is, therefore, quite reasonable that only one satellite structure is observed in the Ni $2p$ XP spectra of the 1D and discrete Ni complexes.

TABLE III. The energy positions of the Auger lines $E_{1,2}$ and the peak energies of the self-convolution of the valence XP spectra E'_2 for the discrete and 1D Ni complexes and the Ni dihalides. $[E_2 - E_1]$ and $[E'_2 - E_1]$ correspond to the on-site d - d Coulomb interaction energy U .

	Auger		Self-Convolution		
	E_1 (eV)	E_2 (eV)	E'_2 (eV)	$[E_2 - E_1]$ (eV)	$[E'_2 - E_1]$ (eV)
$[\text{NiCl}_2([\text{14}] \text{aneN}_4)]\text{ClO}_4$	842.9		847.9		5.0
$[\text{NiBr}_2([\text{14}] \text{aneN}_4)]\text{ClO}_4$	843.3		849.2		5.9
$[\text{Ni}(\text{chxn})_2\text{Cl}]\text{Cl}_2$	843.2		848.1		4.9
$[\text{Ni}(\text{chxn})_2\text{Br}]\text{Br}_2$	843.0		848.5		5.5
NiCl_2	842.8	847.8	847.2	5.0	4.4
NiBr_2	843.2	848.0	847.5	4.8	4.3

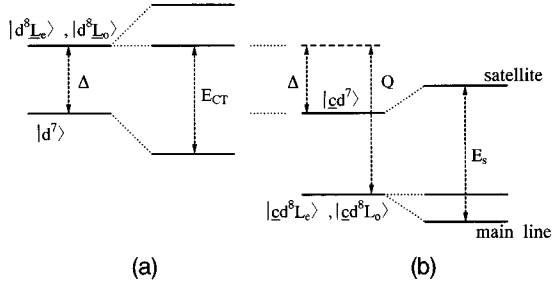


FIG. 6. Schematic energy-level diagram of an isolated trimer ($X\text{-Ni-X}$). (a) and (b) show the neutral state and the core-ionized state, respectively.

To analyze the Ni $2p$ XP spectra of the discrete and 1D Ni complexes, we will consider an $X^-\text{-Ni}^{3+}\text{-X}^-$ trimer, where only the d_{z^2} orbital of the Ni ion and the p_z orbital of the halogen ions are taken into account. The lower-lying state $|d^7\rangle$ and the CT excited states $|d^8\bar{L}_{e,o}\rangle$ are expressed as follows:

$$\begin{aligned} |d^7\rangle &= |X^-\text{Ni}^{3+}\text{X}^- \rangle \\ |d^8\bar{L}_e\rangle &= \frac{1}{\sqrt{2}}(|X^0\text{Ni}^{2+}\text{X}^- \rangle + |X^-\text{Ni}^{2+}\text{X}^0 \rangle) \\ |d^8\bar{L}_o\rangle &= \frac{1}{\sqrt{2}}(|X^0\text{Ni}^{2+}\text{X}^- \rangle - |X^-\text{Ni}^{2+}\text{X}^0 \rangle). \end{aligned} \quad (1)$$

Here Ni^{3+} and X^0 represent a hole in the d_{z^2} orbital and the p_z orbital, respectively, and $|d^8\bar{L}_e\rangle$ and $|d^8\bar{L}_o\rangle$ represent the even (e) CT and odd (o) CT states, respectively. The energy difference between the $|d^7\rangle$ state and the $|d^8\bar{L}_{e,o}\rangle$ states is defined by Δ , and the transfer energy t is defined by

$$\begin{aligned} t &= \langle X^0\text{Ni}^{2+}\text{X}^- | H | X^-\text{Ni}^{3+}\text{X}^- \rangle \\ &= \langle X^-\text{Ni}^{2+}\text{X}^0 | H | X^-\text{Ni}^{3+}\text{X}^- \rangle. \end{aligned} \quad (2)$$

The effective p - d hybridization T is determined as

$$T = \langle d^7 | H | d^8\bar{L}_e \rangle = \sqrt{2}t. \quad (3)$$

As a result of mixing the $|d^7\rangle$ and $|d^8\bar{L}_e\rangle$ states, there are three levels, as shown in Fig. 6(a). Optical-absorption corresponding to the transition from the ground state to the odd CT excited state has the energy $E_{\text{CT}} = \frac{1}{2}(\Delta + \sqrt{\Delta^2 + 4T^2})$.

The next problem is to determine the eigenstates in the presence of a core hole. The final states of the Ni $2p$ XP are composed of $|cd^7\rangle$ and $|cd^8\bar{L}_{e,o}\rangle$ states, the energies of which are E_c and $E_c + \Delta - Q$, respectively. Here c denotes the core-hole state, E_c the core-hole energy relative to the ionic lattice, and Q the core-hole- d -electron Coulomb attraction. In several Ni compounds such as NiO, NiS, and

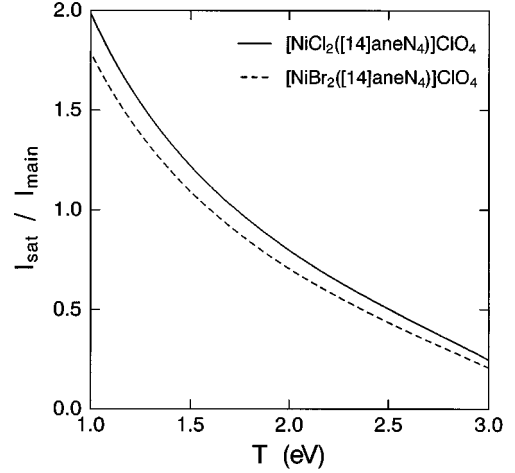


FIG. 7. The ratio of the intensity of the lower-energy satellite and the main line of the Ni $2p_{3/2}$ XP spectra as a function of T in $[\text{NiX}_2([\text{14}]\text{aneN}_4)]\text{ClO}_4$, $X=\text{Cl}$ (the solid line) and $X=\text{Br}$ (the broken line). In the calculations, the parameter values of $E_{\text{CT}} = 3.07$ eV and $E_s = 6.7$ eV are used for $X=\text{Cl}$ and $E_{\text{CT}} = 2.62$ eV and $E_s = 7.0$ eV for $X=\text{Br}$.

La_2NiO_4 , Q is estimated to be $1.2U-1.4U$,³⁰⁻³² which is considerably larger than Δ . Then the energy levels of the final states can be described as Fig. 6(b).

The $|cd^7\rangle$ and $|cd^8\bar{L}_e\rangle$ states are mixed with one another. The resultant two states are responsible for the main line and satellite, as shown in Fig. 6(b). The separation between the satellite and the main line E_s is given as $\sqrt{(\Delta - Q)^2 + 4T^2}$. The relative intensity $I_{\text{sat}}/I_{\text{main}}$ can also be estimated as a function of Δ , T , and Q on the basis of the sudden approximation.

The trimer model can be directly applied to the discrete Ni complexes. From the values of E_{CT} , E_s , and $I_{\text{sat}}/I_{\text{main}}$ experimentally obtained, we can determine the values of Δ , T , and Q . The experimental values of $I_{\text{sat}}/I_{\text{main}}$ include some ambiguity, so that we calculated $I_{\text{sat}}/I_{\text{main}}$ for various values of T in the discrete Ni complexes by using the experimental values of E_{CT} and E_s . ($E_{\text{CT}} = 3.07$ eV and $E_s = 6.7$ eV for $X=\text{Cl}$, and $E_{\text{CT}} = 2.62$ eV and $E_s = 7.0$ eV for $X=\text{Br}$.) The results are plotted in Fig. 7. Using the values of $I_{\text{sat}}/I_{\text{main}}$ ($= 0.55 \pm 0.1$) for the two Ni complexes, we obtained Δ , T , and Q as listed in Table IV. Q/U is 1.1 ± 0.1 ; that is, close to the empirical value 1.2–1.4. The dependence of Δ on the choice of X is in accord with the chemical trend.

In the above discussion, Ni-N hybridization has not been considered. The Ni-N distances is short (less than 2 Å), so that the Ni-N hybridization may not be negligible. However, there is no prominent structure due to the ligand (N) to Ni

TABLE IV. Parameters Δ , T , Q , and U for the discrete Ni complexes and the Ni dihalides.

	Δ	T	Q	U	Ref.
$[\text{NiCl}_2([\text{14}]\text{aneN}_4)]\text{ClO}_4$	1.2 (± 0.3)	2.4 (∓ 0.2)	5.8 (± 0.7)	5.0	This work
$[\text{NiBr}_2([\text{14}]\text{aneN}_4)]\text{ClO}_4$	0.64 (± 0.3)	2.3 (∓ 0.2)	6.0 (± 0.7)	5.9	This work
NiCl_2	3.6	2.8	7.0	5.0	21
NiBr_2	2.6	2.8	7.0	5.0	21

CT transition up to 4 eV in the polarized reflection spectra for $\mathbf{E} \perp \mathbf{b}$ of the 1D Ni complex.² This suggests that the energy levels of the occupied orbitals of the N atoms are much lower than those of the unoccupied d orbitals of the Ni ions. Therefore, the contribution of the atomic orbitals of the N atoms to both the ground and excited states shown in Fig. 6 can be neglected, even if the Ni-N hybridization is comparable with the Ni-X one.

Let us proceed to a discussion of the results of 1D Ni complexes. The trimer model introduced above is too simple to analyze the experimental data of the 1D Ni complexes. However, the parameters Δ , T , and Q estimated for the discrete Ni complexes also seem to be suitable for the 1D Ni complexes, as argued below. The parameters Q and U for the 1D Ni complexes should be nearly equal to those for the discrete Ni complexes, since Q is an atomic quantity. The transfer energy T of the four Ni complexes is determined mainly by the Ni-X distance. As seen in Table I, the difference in Ni-X distances between the discrete Ni complex and the 1D Ni complex with the same halogen ions is negligible (less than 0.04 Å), suggesting that the magnitudes of T in the two types of complexes are almost equal to each other. According to the ionic crystal model, the bare CT gap energy is written as $\Delta = \delta V_M / \varepsilon(\infty) + \Delta_0$,³³ where δV_M is the difference in the Madelung site potentials V_M for holes on the Ni and halogen, $\varepsilon(\infty)$ the dielectric constant, and Δ_0 the atomic limit of the d - p level separation. In the 1D Ni complexes, δV_M will be enhanced by the effect of the long-range Coulomb interaction along the 1D chain. Therefore, Δ of the 1D Ni complex might be slightly larger than that in the discrete Ni complex.

Keeping the above discussions in mind, we will compare the experimental data of the 1D Ni complexes with those of the discrete Ni complexes. E_s and $I_{\text{sat}}/I_{\text{main}}$ of the 1D Ni complexes are not so different from those of the discrete Ni complexes. However, there is a significant difference in E_{CT} ; E_{CT} in the 1D Ni complex is smaller by about 1.3 eV than that in the discrete Ni complex. Such a large decrease of E_{CT} cannot be attributed to the variation in the physical parameters, since T , U , and Q values of the two types of complexes, having the same halogen ions, are almost equal to each other. The possible change in Δ due to the intersite Coulomb interaction in the 1D Ni complex will tend to enhance E_{CT} , contrary to the experimental result, and hence is not responsible for the change of E_{CT} .

The change of E_{CT} is likely explained by taking account of the bandwidths. In 1D Ni complexes, the halogen p_z valence band and the Ni d_{z^2} upper Hubbard band have finite bandwidths which will be comparable with the CT energy because of large T . E_{CT} is generally given as follows:²⁰

$$E_{\text{CT}} = \Delta + (2\delta^n - \delta^{n-1} - \delta^{n+1}) - 1/2(W_p + W_d). \quad (4)$$

Here n is the number of d electrons, δ^n is the hybridization shift, and W_p and W_d are the widths of the p and d bands, respectively. Assuming that the second term of Eq. (4) is common in the two types of complexes, $W (= W_p + W_d)$ in the 1D Ni complexes is estimated to be 2.6 eV from the difference of E_{CT} values for the 1D and discrete complexes.

It is interesting to compare the physical parameters of the discrete and 1D Ni complexes with those of NiX_2 . For NiX_2 , the parameters have been estimated from Ni 2*p* XPS (Refs.

21 and 34) and Ni 3*d* XPS.³⁵ The results obtained by Zaanen, Westra, and Sawatzky from the Ni 2*p* XPS on the basis of the impurity approximation without multiplet effects²¹ are listed in Table IV. They estimated all the parameters (Δ , U , Q , and T) from the Ni 2*p* XP data, but did not reproduce the gap energies (E_{CT}) from these parameters. Because of the difference in the analysis procedure, it is somewhat difficult to compare directly the magnitudes of the parameters between NiX_2 and Ni complexes. Therefore, we shall give only semiquantitative discussions below. As seen in Table IV, the material dependence of U (Ref. 36) and Q is small. As for the p - d hybridization, we should compare the T values defined by $\langle d^7 | H | d^8 \underline{L} \rangle$ for the Ni complexes with those defined by $\langle d^8 | H | d^9 \underline{L} \rangle (= \langle d^9 \underline{L} | H | d^{10} \underline{L}^2 \rangle)$ for NiX_2 .³⁷ T in NiX_2 (2.8 eV) is larger than those in the Ni complexes ($T=2.3$ or 2.4 eV). Such a difference is reflected in the result that the interatomic Auger process is observed in NiX_2 but not in the 1D Ni complexes. The sum of the p - and d -bandwidths W is 3.5 eV ($W_p=3.0$ eV, $W_d=0.5$ eV) in NiX_2 ,²¹ which is larger than that estimated for the 1D Ni complexes ($W=2.6$ eV). In fact, the bandwidths of the valence XP spectra in NiX_2 are larger than those in the 1D Ni complexes as seen in Fig. 3. These results are consistent with the larger p - d hybridizations in NiX_2 as compared with those in 1D Ni complexes. In NiX_2 , the p - p hybridization as well as the p - d one might also be responsible for the larger value of W .

The most remarkable difference between NiX_2 and the 1D Ni complexes is observed in Δ . Δ in the Ni complexes is smaller by about 2 eV than that in NiX_2 . This feature is related to the change in the gap energy E_{CT} ; in the 1D Ni complexes, E_{CT} is 1.8 eV for $X=\text{Cl}$ and 1.3 eV for $X=\text{Br}$, while, in NiX_2 , it is 4.3 eV for $X=\text{Cl}$ and 3.5 eV for $X=\text{Br}$.³⁸ Such a difference in Δ is attributable to the difference in the valency of the metals. As the number of d electrons decreases, the averaged energy of the 3*d* orbitals is lowered, leading to a decrease in the magnitude of Δ . This trend has been clearly observed for the Mn, Fe, or Cu oxides, in which Δ decreases by 2–4 eV from d^n to d^{n-1} .²⁹

Finally, we will discuss the difference in the electronic structures in the Ni and Pt complexes. All of the Pt complexes obtained are in the commensurate CDW state, in which the gap is formed between the filled d_{z^2} (Pt^{2+}) state and the unoccupied d_{z^2} (Pt^{4+}) state. The gap energies of the Pt complexes are 0.85–3.2 eV,^{3,7,8} while the transition energies from the filled p_z state to the unoccupied d_{z^2} state are 5–6 eV.⁵ As for U , several groups have reported the estimated values for Pt to be in the range of 0.5–1 eV.^{4,15,17} Thus U of Pt is much smaller than that of Ni obtained in this paper. Consequently, the CDW state could be stabilized in the Pt complexes by the presence of strong e - l interaction. When replacing Pt by Pd, the enhancement of U is estimated to be about 0.4 eV,^{3,8} which is not so large. Therefore, the Pd complexes are considered to be in the same situation. On the other hand, in the Ni complexes, the CDW state is located at high energy because of the large U , and should be unstable.

VI. CONCLUSION

We have studied the electronic structure of the 1D Ni complexes $[\text{Ni}(\text{chxn})_2\text{X}]_2$ ($X=\text{Cl}, \text{Br}$) and the discrete Ni complexes $[\text{NiX}_2([\text{14}] \text{aneN}_4)]\text{ClO}_4$ ($X=\text{Cl}, \text{Br}$) by use of

optical, XP, and Auger spectroscopies. The CT energy Δ and the transfer energy T of these Ni complexes have been estimated on the basis of the simple trimer model. The average values of the on-site d - d Coulomb interaction energy U have been also evaluated for both the Ni complexes and Ni dihalides. The results demonstrate that 1D Ni complexes are CT insulators similar to the Ni dihalides. The difference in the optical gap energies of the 1D Ni complexes and the discrete Ni complexes can be explained by taking account of the p - and d -band-widths. Δ of the 1D Ni complexes is smaller than Δ in the Ni dihalides, which is attributable to an increase of the valency, or a decrease of the average energy of $3d$ electrons. In 1D Ni complexes, the CDW state becomes unstable

due to the large U value (~ 5 eV). This situation is in contrast with those in the 1D Pt and Pd complexes, where the CDW states are located at lower energies due to the smaller U values.

ACKNOWLEDGMENTS

We would like to thank Professor Y. Tokura (Tokyo University), Professor K. Nasu, and Dr. K. Iwano (KEK) for valuable discussions. This work was partly supported by a Grant-in-Aid for Scientific Research from the Ministry of Education, Science and Culture, Japan.

- ¹Y. Wada, T. Mitani, M. Yamashita, and T. Koda, *J. Phys. Soc. Jpn.* **54**, 3143 (1985).
- ²H. Okamoto, T. Mitani, K. Toriumi, and M. Yamashita, *Phys. Rev. B* **42**, 10 381 (1990).
- ³H. Okamoto, T. Mitani, K. Toriumi, and M. Yamashita, *Mater. Sci. Eng. B* **13**, L9 (1992).
- ⁴K. Nasu, *J. Phys. Soc. Jpn.* **52**, 3865 (1984).
- ⁵Y. Wada, T. Mitani, M. Yamashita, and T. Koda, *J. Phys. Soc. Jpn.* **58**, 3013 (1989).
- ⁶H. Okamoto, T. Mitani, K. Toriumi, and M. Yamashita, *Phys. Rev. Lett.* **69**, 2248 (1992).
- ⁷H. Okamoto, Y. Oka, T. Mitani, K. Toriumi, and M. Yamashita, *Mol. Cryst. Liq. Cryst.* **256**, 161 (1994).
- ⁸H. Okamoto and T. Mitani, *Prog. Theor. Phys.* **113**, 191 (1993).
- ⁹N. Kuroda, M. Sakai, Y. Nishina, M. Tanaka, and S. Kurita, *Phys. Rev. Lett.* **58**, 2122 (1987).
- ¹⁰S. Kurita, M. Haruki, and K. Miyagawa, *J. Phys. Soc. Jpn.* **57**, 1789 (1988).
- ¹¹K. Nasu, *J. Phys. Soc. Jpn.* **53**, 302 (1984), **53**, 427 (1984).
- ¹²D. Baeriswyl and A. R. Bishop, *J. Phys. C* **21**, 339 (1988).
- ¹³A. Mishima and K. Nasu, *Phys. Rev. B* **39**, 5758 (1989); **39**, 5763 (1989).
- ¹⁴Y. Tagawa and N. Suzuki, *J. Phys. Soc. Jpn.* **59**, 4074 (1990).
- ¹⁵K. Iwano and K. Nasu, *J. Phys. Soc. Jpn.* **61**, 1380 (1992).
- ¹⁶J. T. Gammel, A. Saxena, I. Batistic, A. R. Bishop, and S. R. Phillpot, *Phys. Rev. B* **45**, 6408 (1992).
- ¹⁷S. M. Webber-Milbrodt, J. T. Gammel, A. R. Bishop, and E. Y. Lor, Jr., *Phys. Rev. B* **45**, 6435 (1992).
- ¹⁸K. Toriumi, Y. Wada, T. Mitani, S. Bandow, M. Yamashita, and Y. Fujii, *J. Am. Chem. Soc.* **111**, 2341 (1989).
- ¹⁹K. Toriumi, H. Okamoto, T. Mitani, S. Bandow, M. Yamashita, Y. Wada, Y. Fujii, R. J. H. Clark, D. J. Michael, A. J. Edward, D. Watkin, M. Kurmoo, and P. Day, *Mol. Cryst. Liq. Cryst.* **181**, 333 (1990).
- ²⁰J. Zaanen, G. A. Sawatzky, and J. W. Allen, *Phys. Rev. Lett.* **55**, 418 (1985).
- ²¹J. Zaanen, C. Westra, and G. A. Sawatzky, *Phys. Rev. B* **33**, 8060 (1986).
- ²²E. S. Gore and D. H. Busch, *Inorg. Chem.* **12**, 1 (1973).
- ²³K. Toriumi *et al.* (unpublished).
- ²⁴T. Ito, M. Sugimoto, K. Toriumi, and H. Ito, *Chem. Lett.* 1477 (1981).
- ²⁵H. Okamoto, K. Okaniwa, T. Mitani, K. Toriumi, and M. Yamashita, *Solid State Commun.* **77**, 465 (1991).
- ²⁶J. J. Yeh and I. Lindau, *At. Data Nucl. Data Tables* **32**, 1 (1985).
- ²⁷J. J. Larder, *Phys. Rev.* **91**, 1382 (1953).
- ²⁸S. R. Barman, A. Chainani, and D. D. Sarma, *Phys. Rev. B* **49**, 8475 (1994).
- ²⁹A. Chainani, M. Mathew, and D. D. Sarma, *Phys. Rev. B* **46**, 9976 (1992); **48**, 14 818 (1993).
- ³⁰M. Nakamura, A. Fujimori, M. Sacchi, J. C. Fuggle, A. Misu, T. Mamori, H. Tamura, M. Matoba, and S. Anzai, *Phys. Rev. B* **48**, 16 942 (1993).
- ³¹A. E. Bocquet, T. Mizokawa, T. Saitoh, H. Namatame, and A. Fujimori, *Phys. Rev. B* **46**, 3771 (1992).
- ³²H. Eisaki, S. Uchida, T. Mizokawa, H. Namatame, A. Fujimori, J. van Elp, P. Kuiper, G. A. Sawatzky, S. Hosoya, and H. Katayama-Yoshida, *Phys. Rev. B* **45**, 12 513 (1992).
- ³³Y. Ohta, T. Tohyama, and S. Maekawa, *Phys. Rev. Lett.* **66**, 1228 (1991).
- ³⁴K. Okada and A. Kotani, *J. Phys. Soc. Jpn.* **60**, 772 (1991).
- ³⁵K. Okada and T. Jo, *J. Phys. Soc. Jpn.* **61**, 3837 (1992).
- ³⁶ U ($=5$ eV) obtained by Zaanen, Westra, and Sawatzky (Ref. 21) is based upon the model without multiplet effects. As discussed in Ref. 34, when taking account of the intra-atomic multiplet coupling, the larger value of U is generally obtained, e.g., 6.5 eV in NiX_2 ($X=F, Cl, \text{ and } Br$) (Ref. 34) and 7.3 eV in $NiCl_2$ and NiO (Ref. 35). The U values of the Ni complexes (~ 5 eV) evaluated from the Auger spectra in this paper reflect the averaged energy of the d - d Coulomb interaction and hence are close to the value of Zaanen, Westra, and Sawatzky.
- ³⁷In Ref. 21, T is defined by $T=1/\sqrt{2}\langle d^8|H|d^9L\rangle = 1/\sqrt{2}\langle d^9L|H|d^{10}L^2\rangle$. Therefore, the values of $\sqrt{2}T$ reported in Ref. 21 are listed as the effective p - d hybridization for NiX_2 in Table IV.
- ³⁸I. Pollini, J. Thomas, G. Jezequel, J. C. Lecomnier, and R. Mamy, *Phys. Rev. B* **27**, 1303 (1983).